

# Geophysical Research Letters<sup>®</sup>

## RESEARCH LETTER

10.1029/2024GL112887

## Global Climatology of the Daytime Surface Cooling of Urban Parks Using Satellite Observations



### Key Points:

- The global average daytime surface park cool island intensity is 1.5°C based on satellite data from 2,083 parks for the period 2013–2022
- Park cooling varies widely, controlled by park characteristics, background climate, weather conditions, and the surrounding urban form
- Forested parks exhibit the strongest daytime cooling effect and are most resilient to drought conditions

### Supporting Information:

Supporting Information may be found in the online version of this article.

### Correspondence to:

I. Agathangelidis,  
[iliasaga@phys.uoa.gr](mailto:iliasaga@phys.uoa.gr)



### Citation:

Agathangelidis, I., Blougouras, G., Cartalis, C., Polydoros, A., Tzani, C. G., & Philippopoulos, K. (2025). Global climatology of the daytime surface cooling of urban parks using satellite observations. *Geophysical Research Letters*, 52, e2024GL112887. <https://doi.org/10.1029/2024GL112887>

Received 4 OCT 2024  
 Accepted 16 NOV 2024

### Author Contributions:

**Conceptualization:** Ilias Agathangelidis, Georgios Blougouras, Constantinos Cartalis  
**Formal analysis:** Ilias Agathangelidis, Georgios Blougouras  
**Funding acquisition:** Constantinos Cartalis  
**Methodology:** Ilias Agathangelidis, Georgios Blougouras, Constantinos Cartalis  
**Software:** Ilias Agathangelidis, Georgios Blougouras  
**Visualization:** Ilias Agathangelidis  
**Writing – original draft:** Ilias Agathangelidis

Ilias Agathangelidis<sup>1</sup> , Georgios Blougouras<sup>2,3,4</sup>, Constantinos Cartalis<sup>1</sup>, Anastasios Polydoros<sup>1</sup>, Chris G. Tzani<sup>1</sup> , and Konstantinos Philippopoulos<sup>1</sup>

<sup>1</sup>Department of Physics, National and Kapodistrian University of Athens, Athens, Greece, <sup>2</sup>Department of Biogeochemical Integration, Max Planck Institute for Biogeochemistry, Jena, Germany, <sup>3</sup>ELLIS Unit Jena, Jena, Germany, <sup>4</sup>Department of Geography, Friedrich Schiller University Jena, Jena, Germany

**Abstract** Green infrastructure-based heat mitigation strategies can help alleviate the overheating burden on urban residents. While the cooling effect of parks has been explored in individual satellite-based studies, a global, multi-year investigation has been lacking. This study provides a comprehensive global assessment of the daytime surface park cool island (*SPCI*) climatology, using land surface temperatures from 2,083 systematically selected parks worldwide (2013–2022). Through detailed park selection and data stratification, the key drivers influencing the observed *SPCI* intensity are isolated. The analysis reveals that cooling is strongly linked to park type, with well-treed parks being, on average, 3.4°C, cooler than the surrounding urban area during summer. It is further investigated how *SPCI* is influenced by seasonal variations, droughts, and urban morphology across diverse background climates. These findings, along with the developed global *SPCI* data set, offer critical insights for designing climate-resilient green spaces.

**Plain Language Summary** Green infrastructure can help address the heat-related challenges faced by urban populations. In this paper, we examine the ability of urban parks to provide cooling to the warmer adjacent built-up environment. To achieve this, we analyzed land surface temperatures across more than 2,000 parks worldwide, and found that parks act as localized cool spots, with an average daytime temperature difference of 1.5°C compared to their surroundings. Our results also reveal that different park types have greatly varying cooling potential. For instance, parks with a high density of trees can be over 4°C cooler than nearby urban areas, while parks with low vegetation provide less daytime cooling. Additionally, we investigate how broader climatic conditions, drought events, and urban characteristics influence the cooling intensity of parks, aiming to better understand how parks can help mitigate urban overheating under different scenarios.

## 1. Introduction

The combined effects of urbanization and climate change are projected to further exacerbate urban overheating in coming decades, leading to significant impacts on thermal comfort and increasing the risk of heat-related physiological stress (Nazarian et al., 2022). Vegetation has been consistently shown to mitigate air and surface temperatures in urbanized areas (Bowler et al., 2010; Liu et al., 2023; Wong et al., 2021), despite often unfavorable growing conditions and stress factors for plants, such as water shortage and pollutant loading (Konarska et al., 2016; Oke, 1989).

Urban parks exhibit a characteristic set of radiative, thermal and moisture properties, resulting in a distinct surface energy balance. During the day, vegetated parks have significantly slower warming rates than their urban surroundings. This can be primarily attributed to (Oke, 1989): (a) available energy being preferentially channeled into evapotranspiration, and (b) reduced radiant absorption due to shading and the typically higher albedo of vegetation compared to built-up materials. These differences between parks and their urban surrounding give rise to the park cool island (*PCI*) phenomenon (Oke et al., 2017), where within-park temperatures are lower than in the surrounding urban environment (Bowler et al., 2010; Wong et al., 2021).

Using remote sensing data, the thermal regime of parks can be assessed through Land Surface Temperature (*LST*) observations, enabling repetition over time, consistency, and extensive spatial coverage. Specifically focusing on the surface park cool island (*SPCI*) effect, defined as the surface temperature difference between a park and its urban surrounding environment, its characteristics have been assessed through several satellite-based studies (Liu

© 2025. The Author(s).

This is an open access article under the terms of the [Creative Commons Attribution-NonCommercial-NoDeriv](https://creativecommons.org/licenses/by/4.0/) License, which permits use and distribution in any medium, provided the original work is properly cited, the use is non-commercial and no modifications or adaptations are made.

**Writing – review & editing:**

Ilias Agathangelidis,  
Georgios Blougouras,  
Constantinos Cartalis,  
Anastasios Polydoros, Chris G. Tzaniis,  
Konstantinos Philippopoulos

et al., 2023) (Table S1 in Supporting Information S1). Reported daytime *SPCI* intensities vary greatly, from 0.5°C up to 7°C. *SPCI* observations thus far, have been indicative of the cooler surface thermal regime of parks; however, most previous studies have focused on one or few cities and/or have used a limited number of remotely sensed scenes (Table S1 in Supporting Information S1). In addition, there is a relatively constrained geographic scope in previous studies, mostly toward specific types of climatic regimes (Liu et al., 2023). Furthermore, the differentiation of cooling intensity among climate zones (Geng et al., 2022; Zheng et al., 2022; Zhou et al., 2022), across latitudes (Geng et al., 2022; Yu & Hien, 2006; Zhou et al., 2022), and under extreme conditions (Du et al., 2022; Han et al., 2023) remains inconclusive (Liu et al., 2023). Except for the lack of global coverage, such discrepancies may also be attributed to the non-homogeneous definition of *SPCI* intensity that has been used previously across studies (Liu et al., 2023) and/or to different approaches for *LST* retrieval. Another complication arises from the strong dependence of derived *SPCI* intensities on the nature of the urban surroundings. Yet, previous studies have given little consideration to accounting for the presence of other greenspaces in the vicinity of the park or to using a standardized framework, such as the Local Climate Zones (LCZ) classification (I. D. Stewart & Oke, 2012), to describe the surrounding built-up area. These challenges prevent a robust quantitative understanding of the surface cooling efficacy of urban parks, which in turn limits informed and effective climate-sensitive urban design (Santamouris et al., 2018).

To address these key limitations in understanding park cooling, this study introduces the first global *SPCI* climatology. Employing rigorous stratification and experimental control, we explore the influence of park characteristics, geographic location, and climate conditions on *SPCI* for over 2,000 comprehensively selected parks across 371 global cities. This study uniquely combines: (a) global coverage, (b) multi-year and all-season satellite observations, (c) standardized and controlled park selection criteria, (d) classification of parks by vegetation types, (e) the use of LCZs to characterize the surrounding urban environment, and (f) assessment of *SPCI* intensity under extreme conditions, in order to systematically account for confounding factors and offer transferable and actionable insights. Finally, by making all data and results openly accessible we aim to facilitate further research and practical applications in sustainable urban development.

## 2. Data and Methods

### 2.1. Surface Park Cool Island Intensity

For *LST*, the Landsat 8 Level 2 *LST* product is used (Text S1 in Supporting Information S1), accessed through the Google Earth Engine platform (Gorelick et al., 2017) for the years 2013–2022. All Landsat 8 bands are provided at 30 m spatial resolution; thermal bands are provided resampled from an initial 100 m resolution. The pixels with clouds are masked using the Quality Assessment band; if any single pixel within a given park border is masked, the specific date is excluded from our analysis. The Normalized Difference Vegetation Index (*NDVI*) is computed within parks, using the Landsat 8 OLI visible and near-infrared bands.

The *SPCI* intensity is derived as the park-neighborhood *LST* difference (Cao et al., 2010) (Text S2 in Supporting Information S1):

$$SPCI = LST_{urban} - LST_{park} \quad (1)$$

where  $LST_{urban}$  is the mean *LST* within a 500-m buffer zone from the park border and  $LST_{park}$  is the mean *LST* inside the park. Positive (negative) *SPCI* intensity indicates a cooling (warming) effect of parks.

### 2.2. Selection of Parks

A multi-stage approach is employed (Figure S1 and Text S3 in Supporting Information S1) to systematically sample the parks used in this study. First, all available park boundaries are extracted from the open crowd-sourced OpenStreetMap (OSM) platform (OpenStreetMap contributors, 2022) for cities with over 500,000 inhabitants. Parks are then filtered based on their area, with a minimum size of  $100 \times 100 \text{ m}^2$  (1 ha) to ensure adequate capture by the thermal sensor. Sites tagged as parks in OSM, but are mostly non-vegetated, are excluded, retaining only parks with a Landsat-based *NDVI* value higher than the mean *NDVI* minus half standard deviation for all parks in a given city (Text S3 Supporting Information S1). At the following stage of the park sampling process, a semi-

automatic screening procedure is derived in order to isolate and study the cooling effect of parks without unwanted influences from other greenspace in the vicinity. For each park, the pixels inside the 500-m adjacent buffer zone of the park are classified as “impervious” and “non-impervious”, using all unfiltered OSM park boundaries and the Global Artificial Impervious Areas (GAIA) data set (Gong et al., 2020). Then, a maximum threshold value of 5% is set for the non-impervious pixels inside the buffer zone around parks. Next, for parks that meet the above criterion, high-resolution Google Earth images are inspected and the parks that include other parkland or extended natural surfaces in their 500-m buffer zone, not captured by the OSM and GAIA data sets, are further dropped. To minimize further confounding effects and focus solely on vegetation characteristics, parks containing lakes or other inland water bodies are also not included.

After completing all filtering steps, the final data set of parks comprises a total of 2,083 parks in 371 cities (Figure S2 in Supporting Information S1). Using the Köppen—Geiger climate classification (Peel et al., 2007) parks are categorized into four climate zones (tropical, arid, temperate, and cold) and 20 further climate sub-types. Next, high-resolution Google Earth images and ground-level photographs of the parks are visually inspected to classify them into park types based on the categorization proposed by Spronken-Smith and Oke (1998): (a) forest, (b) mixed (parks with a combination of trees and open grass spaces), (c) grass, (d) soil and shrubs, and (e) multi-use parks (parks that include extended impervious surfaces, such as sports fields) (Text S4 and Table S2 in Supporting Information S1). The surrounding urban neighbourhoods of parks is characterized using the LCZ framework (I. D. Stewart & Oke, 2012), which classifies urban sites depending on their urban form and function (Text S5 and Table S3 in Supporting Information S1). A global LCZ product (Demuzere et al., 2022a, 2022b) is used, representative for the nominal year 2018. The percentage of each LCZ class included within the 500-m buffer of each park is computed. The surrounding urban area of a park is classified to a LCZ class only when >50% of the pixels inside the 500-m buffer belong to that class.

### 3. Results

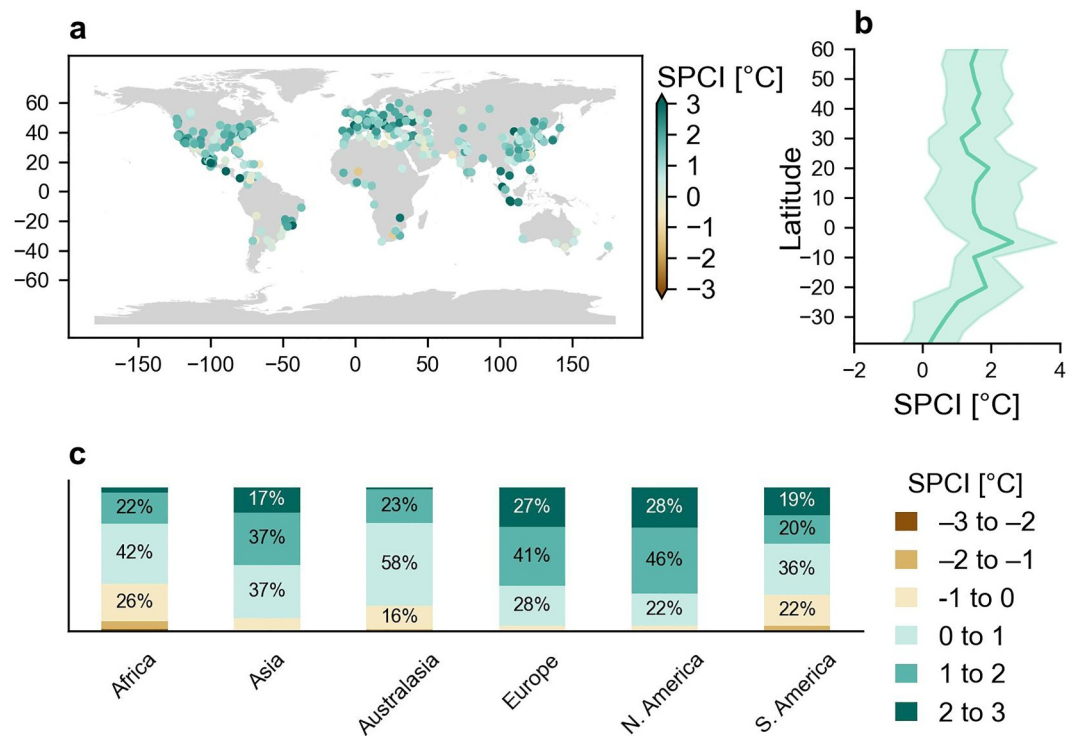
#### 3.1. Global Spatial Variations of the Park Cooling Effect

Figure 1 shows the spatial patterns of annual mean daytime *SPCI* intensity across 2,083 global parks. We find that the global mean *SPCI* is 1.47 (1.42, 1.51)°C; values in the parenthesis define the 95% confidence interval hereafter. *SPCI* is positive over most cities; the great majority of the parks (81%) show a *SPCI* intensity between 0.5 and 3.5°C, with only 7% of the parks being on average warmer than their urban surrounds. The higher annual mean cooling tends to occur near the equator; parks in tropical cities exhibit a *SPCI* of 1.83 (1.63, 2.02)°C (Figure 1b). As can be seen in Figure 1b, the latitudinal pattern is not symmetrical between the two hemispheres; the overall *SPCI* intensity in the Northern Hemisphere (1.55 (1.51, 1.60)°C, number of parks: 1848), is statistically significantly larger ( $p < 0.001$ ,  $t$ -test) than the cooling intensities observed in the Southern Hemisphere (0.78 (0.63, 0.93)°C, number of parks: 235). Differences are also statistically significant ( $p < 0.001$ , ANOVA) by continent; *SPCI* is most pronounced in North America (1.71 (1.65, 1.77)°C), followed by Europe (1.52 (1.43, 1.62)°C) (Figure 1c, Figure S3 in Supporting Information S1).

The park-induced coolness is next examined in relation to the urban form and function characteristics (i.e., the LCZ class) of the urban surrounding area (Table S3 in Supporting Information S1). Overall, parks embedded within closely packed LCZ neighborhoods (high-rise LCZ 1, mid-rise LCZ 2, and low-rise LCZ 3) and the open built LCZ 8 class (which corresponds mainly to industrial and commercial sites) exhibit a higher *SPCI* intensity than parks located in well-vegetated residential areas (LCZ 4–6) (Text S6 in Supporting Information S1).

#### 3.2. Seasonal Cooling Cycle in Relation to Different Background Climates

Next, the park effect alters in response to different climate regimes is assessed. We find that the mean cooling influence is widespread across climate types with small but statistically significant ( $p = 0.024$ , ANOVA) differentiations among them (Figure 2a). The mean annual *SPCI* intensity is highest for cities in the tropics (Köppen-Geiger type A) (1.57 (1.33, 1.80)°C) and lowest for the arid (B) climate type (1.37 (1.26, 1.48)°C). It is shown that *SPCI* displays distinct seasonal patterns across background climates (Figure 2b, Figures S4 and S5 in Supporting Information S1). As the tropics are characterized by a high net radiation flux and ample precipitation year-round, high evapotranspiration can be sustained. Thus, a relatively seasonally stable, moderate park cooling effect is observed in hot and humid cities, ranging from 1.1°C to 2°C.



**Figure 1.** Global spatial variation of daytime surface park cool island intensity. (a) Spatial patterns of annual daytime mean *SPCI* intensity (°C) (averaged per city), where positive (negative) values indicate a cooling (warming) effect of parks. (b) Latitudinal variations of *SPCI* intensity (°C) (averaged per 5 degrees of latitude). The shaded area corresponds to one standard deviation. (c) Discrete distributions of *SPCI* intensity (°C) per continent.

In contrast to tropical cities, the *SPCI* intensity varies more drastically throughout the year in the other climate zones (arid, temperate, and continental). More specifically, for cities in the subtropics and the mid-latitudes, the park-neighborhood temperature difference during the cold season is particularly small (down to < 0.5°C), as evapotranspirative cooling tends to be significantly limited by the lower solar irradiance and lower temperature values, as well as leaf shedding for deciduous trees. In turn, during summer months (when peak plant production typically occurs) parks in arid, temperate and continental climates can create cool islands of at least 2°C, in some

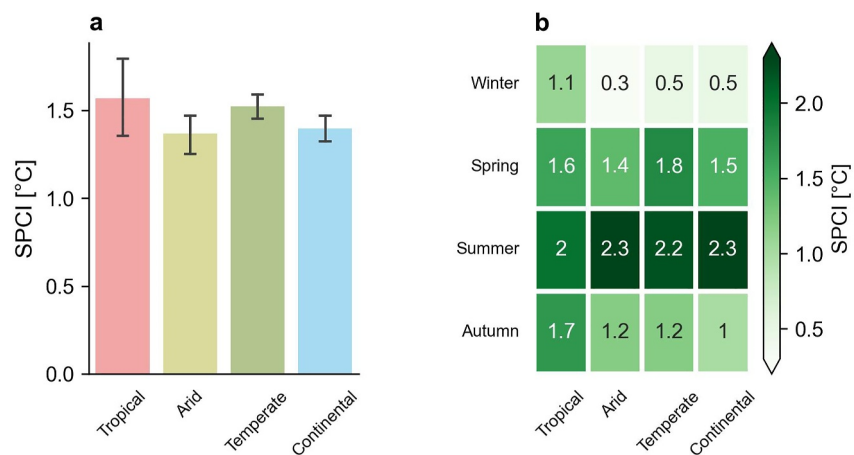


**Figure 2.** The park effect exhibits marked seasonality in most climate zones. (a) Annual daytime mean *SPCI* intensity (°C) in different climate regimes. Error bars indicate the 95% confidence interval. (b) Seasonal variations of *SPCI* intensity (°C) for parks in different background climates.

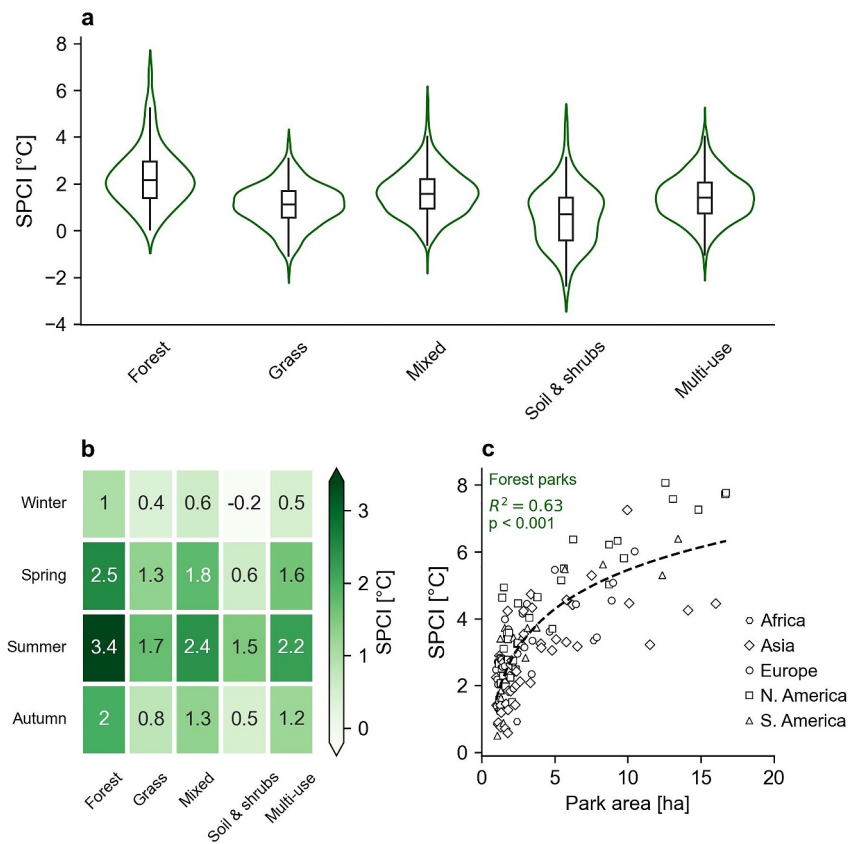


**Figure 3.** Strong dependence of the park cooling effect per park type. (a) Annual daytime mean *SPCI* intensity ( $^{\circ}\text{C}$ ) for parks with differing vegetation type and configuration. The violin plots depict the data distribution through probability density curves derived by a kernel density estimator with a Gaussian kernel. The interior box plots within the violin plots display the 25th and 75th percentiles of *SPCI* intensity, with the middle line representing the 50th percentile. (b) Seasonal variations of annual daytime mean *SPCI* intensity ( $^{\circ}\text{C}$ ) for the different park types. (c) The relationship between the annual daytime mean *SPCI* intensity ( $^{\circ}\text{C}$ ) of forested parks (under 20 ha) and the park area; *SPCI* is averaged over the entire area of each park. Dashed curve corresponds to the fitted logarithmic curve.

cases nearly 5-fold the intensity of winter park cooling values. Moreover, their warm season *SPCI* intensity is found to be slightly greater than the tropics (by approximately  $0.3^{\circ}\text{C}$ ), as for the latter evaporative cooling plateaus, since high air humidity tends to be a limiting factor for evapotranspiration.

Importantly, for all hot and arid climates the difference between the surface temperature of parks and that of the urban surrounds is higher during the summer period when cooling effect is most beneficial for thermal discomfort mitigation, in contrast to the low *SPCI* that occurs during winter months. A marked cooling influence for parks in temperate (Köppen-Geiger type C) climates zones during springtime (*SPCI* intensity of  $1.77$  ( $1.69$ ,  $1.84$ )  $^{\circ}\text{C}$ ) is found, which can be attributed to the favorable conditions (e.g., warmer temperatures, surface moisture availability) for photosynthesis and early leaf emergence. In addition, the *SPCI* intensity for all climate zones (except for the tropics, which as mentioned experience little seasonal variation) tends to be relatively small in autumn. Specific details regarding the park cooling variations across Köppen-Geiger sub-types are provided in Text S7 and Table S5 in Supporting Information S1.

### 3.3. Divergent Cooling Intensities by Park Type

We find that the surface thermal regime of parks is strongly altered by different vegetation characteristics (type and arrangement of vegetation, see Section 2.2) (Figure 3a) ( $p < 0.001$ , ANOVA). *SPCI* intensity is notably higher ( $p < 0.001$ , *t*-test) for well-treed parks compared to the other four categories (mixed, grass, soil and shrubs, and multi-use park types). In particular, forested parks can create substantial cool islands of  $2.30$  ( $2.08$ ,  $2.51$ )  $^{\circ}\text{C}$  (approximately  $3.4^{\circ}\text{C}$  during summer), since daytime parks that are associated with extensive tree canopies attain



maximum cooling benefit through the combined effects of evapotranspiration, shading, and access to water through deeper rooting depths (Spronken-Smith & Oke, 1998). For mixed and multi-use parks moderate *SPCI*s are found, with values of 1.63 (1.55, 1.71)°C and 1.42 (1.36, 1.48)°C respectively. On the other hand, as grassed parks typically have higher daytime warming rates (Spronken-Smith & Oke, 1998), their mean *SPCI* intensity is considerably lower (1.08 (0.98, 1.18)°C) than forested or mixed-vegetation parks. Parks with bare soil ground and/or sparse plant cover (soil and shrubs park type) have a notably low *SPCI* intensity of 0.62 (0.33, 0.91)°C. These pronounced differences among different park types are also evident when we further assess the behavior of the multi-use sub-types ( $p < 0.001$ , ANOVA) (Figure S6 in Supporting Information S1), supporting the robustness of the findings. The park cooling seasonal cycle for the five different park types (Figure 3b) is then considered. It is found that forested parks exhibit significant seasonality, with *SPCI* varying from 1.0°C (winter) to 3.4°C (summer). The lower winter values are attributed to reduced latent heat flux and albedo caused by leaf abscission in deciduous trees during the cold season.

Focusing on well-treed parks during the summer, when their cooling capacity is strongest and the need to mitigate urban overheating is most urgent, the relationship between park size and cooling effect is investigated by developing statistical models. We apply non-linear logarithmic fitting, using the Levenberg-Marquardt algorithm (Moré, 2006), to analyze the influence of park size on cooling intensity (Figure 3c). For small to medium-sized forested parks (<20 ha), the relationship between park size and *SPCI* intensity follows a largely logarithmic pattern, accounting for 62.9% of the variance ( $p < 0.001$ ). Discrepancies in cooling effects observed in parks between 5 and 20 ha can partly be attributed to geographic location (Figure S7 in Supporting Information S1). Beyond 20 ha, the influence of park size on *SPCI* intensity tends to plateau; however, due to the small sample size (only five forested parks between 20 and 50 ha), these results are not statistically significant and not included in the analysis. For other park types, the *SPCI*—park size relationship also exhibits a logarithmic behavior, but with considerably greater uncertainty compared to the robust relationship observed in forested parks.

### 3.4. Drought Sensitivity of Urban Parks

The effect that droughts exert on park cooling is then quantified on the basis of the Standardized Precipitation Index (SPI) based on ERA5-Land data; specific details of the methodology that was followed are given in Text S8 in Supporting Information S1. The difference in the *SPCI* intensity of a park during droughts and typical conditions ( $\Delta SPCI$ ) is computed; a negative value for  $\Delta SPCI$  indicates an adverse drought influence. Across macroclimates, a statistically significant ( $p < 0.001$ ,  $t$ -test) decline of cooling intensity is found during extreme droughts ( $\Delta SPCI_{SPI < -2} = -0.29^\circ\text{C}$ ). On the other hand, park sensitivity to droughts tends to be minimal for the case of severe ( $\Delta SPCI_{SPI(-2, -1.5]} = -0.06^\circ\text{C}$ ) and moderate drought events ( $\Delta SPCI_{SPI(-1.5, -1.0]} = -0.10^\circ\text{C}$ ). We reveal that drought severity plays an important role for parks in cities that are characterized by hot and dry summers (Figure S8 in Supporting Information S1). More specifically, urban parks in arid climates (Köppen-Geiger type B) exhibit a mean decline in *SPCI* intensity of 0.62°C ( $p < 0.001$ ,  $t$ -test) during extreme droughts. A similar behavior is observed in summer for parks in Mediterranean climates with dry summer (Csa, Csb) ( $\Delta SPCI_{SPI < -2} = -0.46^\circ\text{C}$ ) ( $p < 0.001$ ,  $t$ -test). When controlling for the influence of vegetation type on park response, it is observed that forested parks demonstrate strong drought resistance, as they exhibit a negligible difference in *SPCI* intensity between drought and typical conditions. By contrast, the other vegetation types exhibit a  $\Delta SPCI_{SPI < -2}$ , ranging from 0.4 (mixed) to 0.8 (soil and shrubs) for arid and dry climate types.

## 4. Discussion and Conclusions

By conducting a global-scale, multi-year analysis of over 2,000 cities with diverse background climates, this study offers a comprehensive and novel assessment of the *SPCI* climatology and resolves conflicting findings from previous studies regarding background macroclimate. Specifically, prior studies covering multiple climate zones in China had resulted in diverging conclusions, with some studies concluding that cold semi-arid types exhibit the most pronounced cooling effects (Zhou et al., 2022), whereas others indicate higher cooling intensity for humid climates (Geng et al., 2022; Zheng et al., 2022). Results in this work reveal that after controlling for confounding factors the annual *SPCI* intensity globally is highest for parks in tropical regions, while parks in other climates exhibit higher cooling intensity during summer, mainly in response to high vapor pressure deficit. Our analysis demonstrates the significant potential of parks to mitigate urban overheating in arid cities, yet highlights the vulnerability of these areas to drought-induced cooling reductions. Our findings thus challenges previous research that suggested typical minimal cooling benefits for arid climates during summer (C. Wang et al., 2022).

The varying *SPCI* intensities across continents (Figure 1) likely reflect a complex interplay of factors, including differences in background climate and urban morphology. Notably, these contrasts persist even after controlling for these factors, as illustrated for instance in Figure 3c. While an in-depth assessment of human management practices is beyond the scope of the current study, we hypothesize that socioeconomic conditions strongly influence cooling capacity (e.g., through irrigation practices). Importantly, our findings suggest that varying cooling capacity is evident for comparable parks across different countries and socioeconomic contexts and should not be attributed solely to green space availability.

While our estimated average *SPCI* intensities are within the reported ranges of previous studies (Table S1 in Supporting Information S1), our global-scale reveals a pronounced seasonal variability of *SPCI* climatology. While previous studies (Blachowski & Hajnrych, 2021; Yang et al., 2017; Zheng et al., 2022) often focused solely on the warm season, our current analysis reveals that the seasonal variations can exceed 3°C, particularly for high latitude cities. Moreover, we uncover significant differences in seasonal variability across climate zones (Figure 2 and Table S4 in Supporting Information S1) and vegetation types (Figure 3b), challenging the previous notion of absent cooling effects during winter (Zhao et al., 2021).

Moreover, this study introduces a methodological framework to account for the influence of the surrounding urban area on park cooling effects. First, we developed a rigorous, systematic process to globally identify parks free from the cooling influence of nearby parkland or natural surfaces. Next, we characterized the urban neighborhoods around these parks, using the LCZ classification, providing a standardized and systematic approach. While widely used in urban climatology, an LCZ-based approach has not been used for *SPCI* analysis in previous works, with notable exceptions in a single-city case study (Kirschner et al., 2023). Our study thus addressed a critical gap, offering the first standardized characterization of urban surroundings in a global *SPCI* climatology.

The *SPCI* effect shares several similarities with the Surface Urban Heat Island (*SUHI*) in terms of their development and intensity, yet notable differences also emerged in the current work. The peak summer daytime cooling that we find for parks in arid macroclimates (Figure 2b) is consistent with other studies (Larson & Perrings, 2013; Song & Wang, 2015) regarding vegetation in xeric environments, despite the negative daytime *SUHI* that is typically developed for the urban area (Stewart et al., 2021) and its general stable seasonality (Sismanidis et al., 2022). Nevertheless, the cooling effect of evapotranspiration can be limited or even reversed during periods of intense drought. Overall, we observe that the influence of droughts on park cooling is highly dependent on the city background climate. This insight clarifies previously conflicting results in the literature regarding *SPCI* intensity during extreme conditions (Liu et al., 2023). In particular, parks in dry climates, such as the Mediterranean, have a statistically significant reduction in cooling influence at times of extreme drought, aligning with previous findings (Zhao, Meili, et al., 2023). Furthermore, our findings reveal forested parks tend to have better drought response than low-vegetation parks; our results likely reflect drought avoidance traits of trees such as a deep root system (Brown et al., 2015).

Moreover, this study demonstrates that well-treed parks consistently provide greater daytime cooling than other park types, due to the combined effect of evaporative cooling and shading (Figure 3a). The enhanced cooling efficacy of forested parks, previously noted in localized studies (Spronken-Smith & Oke, 1998), is confirmed here on a global scale, underscoring the robustness of this result across various macroclimates and seasons. For small and medium-sized well-treed parks, a robust logarithmic increase in cooling with increasing park area is observed, consistent with findings from previous single-case studies (Qiu & Jia, 2020; Ren et al., 2013; X. Wang et al., 2018), suggesting the potential to generalize local mechanisms controlling the upper limit of cooling. However, due to the small sample size for larger parks, we were unable to confirm whether *SPCI* plateaus beyond a certain park size. Further research is needed to identify the potential upper limit and optimize park design for cost-effective cooling. In addition, numerical simulations could be used to explore cause-and-effect relations in the thermal behavior of parks by isolating specific processes of interest (Meili et al., 2021).

In general, our study on urban parks reinforces the previously observed cooling benefits of urban tree planting, as obtained using remotely sensed *LST* across multiple European (Schwaab et al., 2021) and global (Zhao, Zhao, et al., 2023) cities. We stress, however, that satellite-based observations correspond to an elevated cooling plane in the case of forested parks which may not be directly coupled with the surface air temperature. In addition, satellites cannot provide a “complete” (i.e., 3-D) urban surface temperature (Stewart et al., 2021). Full reporting of site metadata, including park characteristics and built-up environment (LCZ), in our provided data set ensures

transparency and enables accurate interpretation of our results. When assessing green-infrastructure strategies, it is also essential to consider additional effects, such as potential adverse impacts on pedestrian thermal comfort due to increased humidity (Huang et al., 2021)—even if a city under typical conditions form a “dry island” (X. Huang & Song, 2023; Meili et al., 2022). At the same time, reduced radiant load through shading (Rahman et al., 2020) or impacts in the micrometeorology and local wind patterns (Kong et al., 2014) further complicate the net thermal comfort effects of urban trees and parks. Another limitation of our study focusing solely on daytime observations; during nighttime the situation is expected to be reversed, with grassed parks anticipated to be cooler (Spronken-Smith & Oke, 1998) Further studies have the potential to offer valuable insights into the diurnal range of park cooling in relation to park types and should also consider variations in SPCI cooling extent and the factors influencing it.

Synthesizing results from previous local studies into a generalized quantitative understanding of SPCI climatology has been challenging due to lack of unified methodologies, limited satellite scenes, and a constrained geographic scope. By following a standardized methodology and establishing experimental control through site and data stratification, we reveal the temporal and spatial patterns of daytime SPCI intensity, which vary according to park characteristics, climate, season, and urban form. This global-scale analysis, combined with the open data set provided, readily supports the development of site-specific adaptation measures and enhances the comparability and transferability of urban climate knowledge. As demonstrated, vegetated urban parks can robustly provide more heat comfortable environments and reduce heat stress vulnerability; however, their design must consider both current and future climate conditions, along with their resilience during extremes.

### Conflict of Interest

The authors declare no conflicts of interest relevant to this study.

### Data Availability Statement

All data sets are publicly available. The Landsat 8 Level 2 product is available at [https://developers.google.com/earth-engine/datasets/catalog/LANDSAT\\_LC08\\_C02\\_T1\\_L2](https://developers.google.com/earth-engine/datasets/catalog/LANDSAT_LC08_C02_T1_L2). The GAIA data set can be accessed at <http://data.starcloud.pcl.ac.cn/resource/13>. The original park boundaries are available at <https://www.openstreetmap.org>. The LCZ data set is available from Demuzere et al. (2022a, 2022b), and ERA5-Land reanalysis data from Muñoz-Sabater, J. (2019). The SPCI data set produced in this research is publicly available at Agathangelidis et al. (2024).

### References

- Agathangelidis, I., Blougouras, G., Cartalis, C., Polydoros, A., Tzanis, C. G., & Philippopoulos, K. (2024). Supplementary dataset for “global climatology of the daytime surface cooling of urban parks using satellite observations” [Dataset]. *Zenodo*. <https://doi.org/10.5281/zenodo.13879997>
- Blachowski, J., & Hajnrych, M. (2021). Assessing the cooling effect of four urban parks of different sizes in a temperate continental climate zone: Wrocław (Poland). *Forests*, *12*(8), 1136. <https://doi.org/10.3390/f12081136>
- Bowler, D. E., Buyung-Ali, L., Knight, T. M., & Pullin, A. S. (2010). Urban greening to cool towns and cities: A systematic review of the empirical evidence. *Landscape and Urban Planning*, *97*(3), 147–155. <https://doi.org/10.1016/j.landurbplan.2010.05.006>
- Brown, R. D., Vanos, J., Kenny, N., & Lenzholzer, S. (2015). Designing urban parks that ameliorate the effects of climate change. *Landscape and Urban Planning*, *138*, 118–131. <https://doi.org/10.1016/j.landurbplan.2015.02.006>
- Cao, X., Onishi, A., Chen, J., & Imura, H. (2010). Quantifying the cool island intensity of urban parks using ASTER and IKONOS data. *Landscape and Urban Planning*, *96*(4), 224–231. <https://doi.org/10.1016/j.landurbplan.2010.03.008>
- Demuzere, M., Kittner, J., Martilli, A., Mills, G., Moede, C., Stewart, I. D., et al. (2022a). A global map of local climate zones to support earth system modelling and urban-scale environmental science. *Earth System Science Data*, *14*(8), 3835–3873. <https://doi.org/10.5194/essd-14-3835-2022>
- Demuzere, M., Kittner, J., Martilli, A., Mills, G., Moede, C., Stewart, I. D., et al. (2022b). Global map of local climate zones [Dataset]. *Zenodo*, *1.0.0*. <https://doi.org/10.5281/zenodo.6364594>
- Du, C., Jia, W., Chen, M., Yan, L., & Wang, K. (2022). How can urban parks be planned to maximize cooling effect in hot extremes? Linking maximum and accumulative perspectives. *Journal of Environmental Management*, *317*, 115346. <https://doi.org/10.1016/j.jenvman.2022.115346>
- Geng, X., Yu, Z., Zhang, D., Li, C., Yuan, Y., & Wang, X. (2022). The influence of local background climate on the dominant factors and threshold-size of the cooling effect of urban parks. *Science of the Total Environment*, *823*, 153806. <https://doi.org/10.1016/j.scitotenv.2022.153806>
- Gong, P., Li, X., Wang, J., Bai, Y., Chen, B., Hu, T., et al. (2020). Annual maps of global artificial impervious area (GAIA) between 1985 and 2018. *Remote Sensing of Environment*, *236*, 111510. <https://doi.org/10.1016/j.rse.2019.111510>
- Gorelick, N., Hancher, M., Dixon, M., Ilyushchenko, S., Thau, D., & Moore, R. (2017). Google earth engine: Planetary-scale geospatial analysis for everyone. *Remote Sensing of Environment*, *202*, 18–27. <https://doi.org/10.1016/j.rse.2017.06.031>
- Han, D., Xu, X., Qiao, Z., Wang, F., Cai, H., An, H., et al. (2023). The roles of surrounding 2D/3D landscapes in park cooling effect: Analysis from extreme hot and normal weather perspectives. *Building and Environment*, *231*, 110053. <https://doi.org/10.1016/j.buildenv.2023.110053>

### Acknowledgments

This research is supported by the project “Support for upgrading the operation of the National Network for Climate Change (CLIMPACT)” (code no. 2023NA11900001) financed by the Public Investments Program of Greece.



- Huang, X., & Song, J. (2023). Urban moisture and dry islands: Spatiotemporal variation patterns and mechanisms of urban air humidity changes across the globe. *Environmental Research Letters*, 18(10), 103003. <https://doi.org/10.1088/1748-9326/acf7d7>
- Huang, X., Song, J., Wang, C., Chui, T. F. M., & Chan, P. W. (2021). The synergistic effect of urban heat and moisture islands in a compact high-rise city. *Building and Environment*, 205, 108274. <https://doi.org/10.1016/j.buildenv.2021.108274>
- Kirschner, V., Macků, K., Moravec, D., & Mañas, J. (2023). Measuring the relationships between various urban green spaces and local climate zones. *Scientific Reports*, 13(1), 9799. <https://doi.org/10.1038/s41598-023-36850-6>
- Konarska, J., Uddling, J., Holmer, B., Lutz, M., Lindberg, F., Pleijel, H., & Thorsson, S. (2016). Transpiration of urban trees and its cooling effect in a high latitude city. *International Journal of Biometeorology*, 60(1), 159–172. <https://doi.org/10.1007/s00484-015-1014-x>
- Kong, F., Yin, H., Wang, C., Cavan, G., & James, P. (2014). A satellite image-based analysis of factors contributing to the green-space cool island intensity on a city scale. *Urban Forestry and Urban Greening*, 13(4), 846–853. <https://doi.org/10.1016/j.ufug.2014.09.009>
- Larson, E. K., & Perrings, C. (2013). The value of water-related amenities in an arid city: The case of the Phoenix metropolitan area. *Landscape and Urban Planning*, 109(1), 45–55. <https://doi.org/10.1016/j.landurbplan.2012.10.008>
- Liu, H., Huang, B., Cheng, X., Yin, M., Shang, C., Luo, Y., & He, B.-J. (2023). Sensing-based park cooling performance observation and assessment: A review. *Building and Environment*, 245, 110915. <https://doi.org/10.1016/j.buildenv.2023.110915>
- Meili, N., Manoli, G., Burlando, P., Carmeliet, J., Chow, W. T. L., Coutts, A. M., et al. (2021). Tree effects on urban microclimate: Diurnal, seasonal, and climatic temperature differences explained by separating radiation, evapotranspiration, and roughness effects. *Urban Forestry and Urban Greening*, 58, 126970. <https://doi.org/10.1016/j.ufug.2020.126970>
- Meili, N., Paschalis, A., Manoli, G., & Faticchi, S. (2022). Diurnal and seasonal patterns of global urban dry islands. *Environmental Research Letters*, 17(5), 054044. <https://doi.org/10.1088/1748-9326/ac68f8>
- More, J. J. (2006). The Levenberg-Marquardt algorithm: Implementation and theory. In *Numerical analysis: Proceedings of the biennial conference held at dundee, June 28–July 1, 1977* (pp. 105–116). Springer.
- Muñoz-Sabater, J. (2019). ERA5-Land hourly data from 1950 to present. Copernicus Climate Change Service (C3S) [Dataset]. *Climate Data Store (CDS)*. <https://doi.org/10.24381/cds.e2161bac>
- Nazarian, N., Krayenhoff, E. S., Bechtel, B., Hondula, D. M., Paolini, R., Vanos, J., et al. (2022). Integrated assessment of urban overheating impacts on human life. *Earth's Future*, 10(8), e2022EF002682. <https://doi.org/10.1029/2022EF002682>
- Oke, T. R. (1989). The micrometeorology of the urban forest. *Philosophical Transactions of the Royal Society of London B Biological Sciences*, 324(1223), 335–349.
- Oke, T. R., Mills, G., Christen, A., & Voogt, J. A. (2017). *Urban climates*. Cambridge University Press.
- OpenStreetMap contributors. (2022). Planet dump. Retrieved from <https://www.openstreetmap.org>
- Peel, M. C., Finlayson, B. L., & McMahon, T. A. (2007). Updated world map of the Köppen-Geiger climate classification. *Hydrology and Earth System Sciences*, 11(5), 1633–1644. <https://doi.org/10.5194/hess-11-1633-2007>
- Qiu, K., & Jia, B. (2020). The roles of landscape both inside the park and the surroundings in park cooling effect. *Sustainable Cities and Society*, 52, 101864. <https://doi.org/10.1016/j.scs.2019.101864>
- Rahman, M. A., Hartmann, C., Moser-Reischl, A., von Strachwitz, M. F., Paeth, H., Pretzsch, H., et al. (2020). Tree cooling effects and human thermal comfort under contrasting species and sites. *Agricultural and Forest Meteorology*, 287, 107947. <https://doi.org/10.1016/j.agrformet.2020.107947>
- Ren, Z., He, X., Zheng, H., Zhang, D., Yu, X., Shen, G., & Guo, R. (2013). Estimation of the relationship between urban park characteristics and park cool island intensity by remote sensing data and field measurement. *Forests*, 4(4), 868–886. <https://doi.org/10.3390/f4040868>
- Santamouris, M., Ban-Weiss, G., Osmond, P., Paolini, R., Synnefa, A., Cartalis, C., et al. (2018). Progress in urban greenery mitigation science – Assessment methodologies advanced technologies and impact on cities. *Journal of Civil Engineering and Management*, 24(8), 638–671. <https://doi.org/10.3846/jcem.2018.6604>
- Schwaab, J., Meier, R., Mussetti, G., Seneviratne, S., Bürgi, C., & Davin, E. L. (2021). The role of urban trees in reducing land surface temperatures in European cities. *Nature Communications*, 12(1), 6763. <https://doi.org/10.1038/s41467-021-26768-w>
- Sismanidis, P., Bechtel, B., Perry, M., & Ghent, D. (2022). The seasonality of surface urban heat islands across climates. *Remote Sensing*, 14(10), 2318. <https://doi.org/10.3390/rs14102318>
- Song, J., & Wang, Z.-H. (2015). Impacts of mesic and xeric urban vegetation on outdoor thermal comfort and microclimate in Phoenix, AZ. *Building and Environment*, 94, 558–568. <https://doi.org/10.1016/j.buildenv.2015.10.016>
- Spronken-Smith, R. A., & Oke, T. R. (1998). The thermal regime of urban parks in two cities with different summer climates. *International Journal of Remote Sensing*, 19(11), 2085–2104. <https://doi.org/10.1080/014311698214884>
- Stewart, I. D., Krayenhoff, E. S., Voogt, J. A., Lachapelle, J. A., Allen, M. A., & Broadbent, A. M. (2021). Time evolution of the surface urban heat island. *Earth's Future*, 9(10), e2021EF002178. <https://doi.org/10.1029/2021EF002178>
- Stewart, I. D., & Oke, T. R. (2012). Local climate zones for urban temperature studies. *Bulletin of the American Meteorological Society*, 93(12), 1879–1900. <https://doi.org/10.1175/BAMS-D-11-00019.1>
- Wang, C., Ren, Z., Dong, Y., Zhang, P., Guo, Y., Wang, W., & Bao, G. (2022). Efficient cooling of cities at global scale using urban green space to mitigate urban heat island effects in different climatic regions. *Urban Forestry and Urban Greening*, 74, 127635. <https://doi.org/10.1016/j.ufug.2022.127635>
- Wang, X., Cheng, H., Xi, J., Yang, G., & Zhao, Y. (2018). Relationship between park composition, vegetation characteristics and cool island effect. *Sustainability*, 10(3), 587. <https://doi.org/10.3390/su10030587>
- Wong, N. H., Tan, C. L., Kolokotsa, D. D., & Takebayashi, H. (2021). Greenery as a mitigation and adaptation strategy to urban heat. *Nature Reviews Earth and Environment*, 2(3), 166–181. <https://doi.org/10.1038/s43017-020-00129-5>
- Yang, C., He, X., Yu, L., Yang, J., Yan, F., Bu, K., et al. (2017). The cooling effect of urban parks and its monthly variations in a snow climate city. *Remote Sensing*, 9(10), 1066. <https://doi.org/10.3390/rs9101066>
- Yu, C., & Hien, W. N. (2006). Thermal benefits of city parks. *Energy and Buildings*, 38(2), 105–120. <https://doi.org/10.1016/j.enbuild.2005.04.003>
- Zhao, J., Meili, N., Zhao, X., & Faticchi, S. (2023). Urban vegetation cooling potential during heatwaves depends on background climate. *Environmental Research Letters*, 18(1), 014035. <https://doi.org/10.1088/1748-9326/acaaf0f>
- Zhao, J., Zhao, X., Liang, S., Wang, H., Liu, N., Liu, P., & Wu, D. (2021). Dynamic cooling effects of permanent urban green spaces in Beijing, China. *Remote Sensing*, 13(16), 3282. <https://doi.org/10.3390/rs13163282>
- Zhao, J., Zhao, X., Wu, D., Meili, N., & Faticchi, S. (2023). Satellite-based evidence highlights a considerable increase of urban tree cooling benefits from 2000 to 2015. *Global Change Biology*, 29(11), 3085–3097. <https://doi.org/10.1111/gcb.16667>
- Zheng, S., Liu, L., Dong, X., Hu, Y., & Niu, P. (2022). Dominance of influencing factors on cooling effect of urban parks in different climatic regions. *International Journal of Environmental Research and Public Health*, 19(23), 15496. <https://doi.org/10.3390/ijerph192315496>

Zhou, Y., Zhao, H., Mao, S., Zhang, G., Jin, Y., Luo, Y., et al. (2022). Studies on urban park cooling effects and their driving factors in China: Considering 276 cities under different climate zones. *Building and Environment*, 222, 109441. <https://doi.org/10.1016/j.buildenv.2022.109441>

## References From the Supporting Information

- Alves, E. D. L. (2017). Quantifying the effect of waterways and green areas on the surface temperature. *Acta Scientiarum. Technology*, 39(1), 89–96. <https://doi.org/10.4025/actascitechnol.v39i1.30469>
- Bechtel, B., Demuzere, M., Mills, G., Zhan, W., Sismanidis, P., Small, C., & Voogt, J. (2019). SUHI analysis using local climate zones—A comparison of 50 cities. *Urban Climate*, 28, 100451. <https://doi.org/10.1016/j.uclim.2019.01.005>
- Chakraborty, T., & Lee, X. (2019). A simplified urban-extent algorithm to characterize surface urban heat islands on a global scale and examine vegetation control on their spatiotemporal variability. *International Journal of Applied Earth Observation and Geoinformation*, 74, 269–280. <https://doi.org/10.1016/j.jag.2018.09.015>
- Cheng, X., Wei, B., Chen, G., Li, J., & Song, C. (2015). Influence of park size and its surrounding urban landscape patterns on the park cooling effect. *Journal of Urban Planning and Development*, 141(3), A4014002. [https://doi.org/10.1061/\(ASCE\)UP.1943-5444.0000256](https://doi.org/10.1061/(ASCE)UP.1943-5444.0000256)
- Feyisa, G. L., Dons, K., & Meilby, H. (2014). Efficiency of parks in mitigating urban heat island effect: An example from Addis Ababa. *Landscape and Urban Planning*, 123, 87–95. <https://doi.org/10.1016/j.landurbplan.2013.12.008>
- Foga, S., Scaramuzza, P. L., Guo, S., Zhu, Z., Dilley, R. D., Beckmann, T., et al. (2017). Cloud detection algorithm comparison and validation for operational Landsat data products. *Remote Sensing of Environment*, 194, 379–390. <https://doi.org/10.1016/j.rse.2017.03.026>
- Huang, F., Jiang, S., Zhan, W., Bechtel, B., Liu, Z., Demuzere, M., et al. (2023). Mapping local climate zones for cities: A large review. *Remote Sensing of Environment*, 292, 113573. <https://doi.org/10.1016/j.rse.2023.113573>
- Imhoff, M. L., Zhang, P., Wolfe, R. E., & Bounoua, L. (2010). Remote sensing of the urban heat island effect across biomes in the continental USA. *Remote Sensing of Environment*, 114(3), 504–513. <https://doi.org/10.1016/j.rse.2009.10.008>
- Li, H., Wang, G., Tian, G., & Jombach, S. (2020). Mapping and analyzing the park cooling effect on urban heat island in an expanding city: A case study in Zhengzhou city, China. *Land*, 9(2), 57. <https://doi.org/10.3390/land9020057>
- Li, K., Chen, Y., & Gao, S. (2022). Uncertainty of city-based urban heat island intensity across 1112 global cities: Background reference and cloud coverage. *Remote Sensing of Environment*, 271, 112898. <https://doi.org/10.1016/j.rse.2022.112898>
- Lin, W., Yu, T., Chang, X., Wu, W., & Zhang, Y. (2015). Calculating cooling extents of green parks using remote sensing: Method and test. *Landscape and Urban Planning*, 134, 66–75. <https://doi.org/10.1016/j.landurbplan.2014.10.012>
- Malakar, N. K., Hulley, G. C., Hook, S. J., Laraby, K., Cook, M., & Schott, J. R. (2018). An operational land surface temperature product for Landsat thermal data: Methodology and validation. *IEEE Transactions on Geoscience and Remote Sensing*, 56(10), 5717–5735. <https://doi.org/10.1109/TGRS.2018.2824828>
- McKee, T. B., Doesken, N. J., & Kleist, J., & others. (1993). The relationship of drought frequency and duration to time scales. *Proceedings of the 8th conference on applied climatology*, 17, 179–183.
- Muñoz-Sabater, J., Dutra, E., Agustí-Panareda, A., Albergel, C., Arduini, G., Balsamo, G., et al. (2021). ERA5-Land: A state-of-the-art global reanalysis dataset for land applications. *Earth System Science Data*, 13(9), 4349–4383. <https://doi.org/10.5194/essd-13-4349-2021>
- Peng, S., Piao, S., Ciais, P., Friedlingstein, P., Otle, C., Bréon, F.-M., et al. (2012). Surface urban heat island across 419 global Big cities. *Environmental Science and Technology*, 46(2), 696–703. <https://doi.org/10.1021/es2030438>
- Roth, M. (2007). Review of urban climate research in (sub)tropical regions. *International Journal of Climatology*, 27(14), 1859–1873. <https://doi.org/10.1002/joc.1591>
- Schneider, A., Friedl, M. A., & Potere, D. (2009). A new map of global urban extent from MODIS satellite data. *Environmental Research Letters*, 4(4), 044003. <https://doi.org/10.1088/1748-9326/4/4/044003>
- Sims, K., Reith, A., Bright, E., McKee, J., & Rose, A. (2022). *LandScan global 2021*. Oak Ridge National Laboratory. <https://doi.org/10.48690/1527702>
- Skarbit, N., Stewart, I. D., Unger, J., & Gál, T. (2017). Employing an urban meteorological network to monitor air temperature conditions in the ‘local climate zones’ of Szeged, Hungary. *International Journal of Climatology*, 37(S1), 582–596. <https://doi.org/10.1002/joc.5023>
- Stewart, I. D., & Mills, G. (2021). *The urban heat island*. Elsevier.
- Xia, H., Chen, Y., Song, C., Li, J., Quan, J., & Zhou, G. (2022). Analysis of surface urban heat islands based on local climate zones via spatiotemporally enhanced land surface temperature. *Remote Sensing of Environment*, 273, 112972. <https://doi.org/10.1016/j.rse.2022.112972>
- Xie, Q., & Li, J. (2021). Detecting the cool island effect of urban parks in Wuhan: A city on rivers. *International Journal of Environmental Research and Public Health*, 18(1), 132. <https://doi.org/10.3390/ijerph18010132>
- Yang, Q., Huang, X., Yang, J., & Liu, Y. (2021). The relationship between land surface temperature and artificial impervious surface fraction in 682 global cities: Spatiotemporal variations and drivers. *Environmental Research Letters*, 16(2), 024032. <https://doi.org/10.1088/1748-9326/abdaed>
- Yao, X., Yu, K., Zeng, X., Lin, Y., Ye, B., Shen, X., & Liu, J. (2022). How can urban parks be planned to mitigate urban heat island effect in “Furnace cities”? An accumulation perspective. *Journal of Cleaner Production*, 330, 129852. <https://doi.org/10.1016/j.jclepro.2021.129852>